## EXCITED-STATE MIXING OF SODIUM ATOMS
## BY COLLISIONS WITH NOBLE-GAS-ATOMS
## AS OBSERVED IN OPTICAL PUMPING EXPERIMENTS EMPLOYING $D_2$ LIGHT

By M. Elbel and W. Schneider
University of Marburg, Federal Republic of Germany

### Introduction to the method

Optical pumping with $D_2$-light can most easily be explained
by using a pumping scheme of a hypothetical alkali atom without
nuclear spin. Fig. 1 shows how optical pumping works in this case.
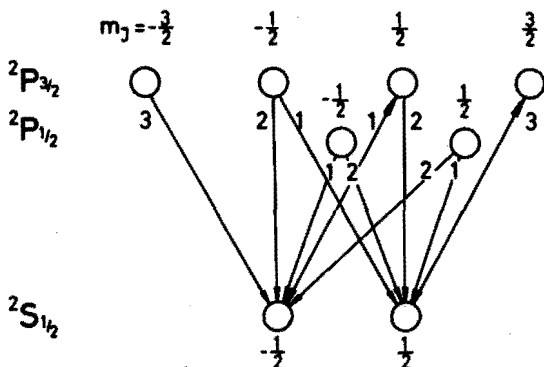Two transitions can be induced with $D_2$-$\sigma^+$-light, but only one is



Fig. 1. Pumping scheme of a hypothetical alkali atom without nuclear spin.
The fine structure components of the excited state are placed one below
other respectively

efficient in optical pumping because any atom excited by the other one goes back the way it is excited. This kind of pumping causes a drop of optical transparency because the stronger absorbing sublevel is populated and the weaker absorbing one is emptied. The situation changes if collision processes occur during the life of the excited state which tend to redistribute the population of the initially excited sublevel among all the six sublevels of the excited state. Then the both exciting transitions become efficient in optical pumping and the stronger absorbing ground state sublevel will be emptied and the weaker one will be filled. Thus pumping has reversed sign. Pumping with high buffer gas pressure which is of course the case of strong excited state mixing will, therefore, cause an increase of optical transparency whereas pumping without buffer gas will cause a decrease. Besides there will be a marked case where optical pumping with $D_2$-light causes no change of optical transparency at all. It can be realized by certain buffer gas pressures. An easy consideration [1, 2] predicts that this case happens if the condition $2 T = 3\tau$ holds, T being the mean collision time, $\tau$ being the mean life of the excited states. This condition may be utilized in order to deduce excited state mixing cross sections from these pressures. This method has to be refined for two reasons. First all the alkaline elements have nuclear spins. Therefore, we have to extend our consideration to a great manifold of hyperfine Zeeman levels. We have to care for all their individual
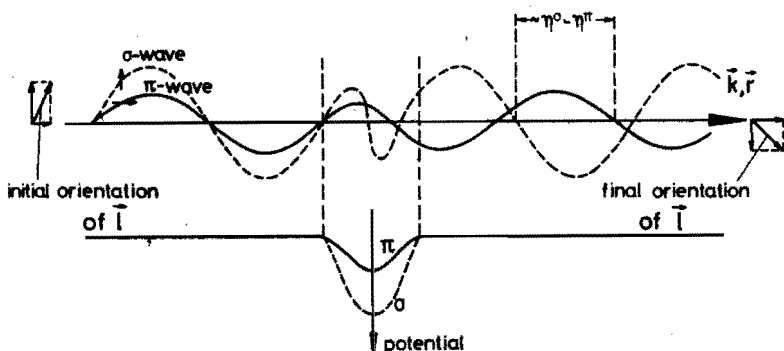


Fig. 2. Model for depolarizing scattering. It is made evident how relative scattering phases concerning the $\sigma$ - and the $\pi$ -state arise

transition probabilities, especially the collision induced ones. Secondly we have to consider that the pumping light has a hyper- fine spectrum which generally differs from a continuum.

## Calculation of relative transition probabilities by means of an almost realistic $m_J$-mixing model

Fig. 2 shows an atom in the state P approaching a noble gas atom. It is initially oriented referring to a certain quantiza- tion axis, for instance the magnetic field of our experiment. The direction of the atoms approach is given by the wave vector $\vec{k}$. This direction is in general different from that one of the quantization axis. Therefore, the wave function of the electron P is a superposition of all the three Zeeman substates when it is referred to the $\vec{k}$-axis whereas it would be a unique Zeeman substate with respect to the quantization axis. The $m_1 = \pm1$-state referring to the $\vec{k}$-axis may be called the molecular $\pi$-state, the $m_1 = 0$-state may be called the molecular $\sigma$-state.* Let us assume that the molecular $\sigma$-states and $\pi$-states experience different potentials during the collision. Therefore, they evolve with different scattering phases from the collision. If we are now re-expanding the outgoing wave to the original quantization axis we shall realize that there are more states present than the initial one. That means transitions occured to other Zeeman substates during the collision.

The scattering amplitude from any initial state j, F; M to any final state j', F', M' is given by the formula (1). It depends on the angles $\beta$, $\gamma$ which describe the orientation of the $\vec{k}$-vector with respect to the initial quantization axis

---

*Note that this is true only in the scope of an one-dimensional scat- tering model where the scattering potential is assumed to be a ditch rather than a hole extending vertically to the $\vec{k}$-vector. In the three-di- mensional case the molecular $\sigma$- and $\pi$-state are to be referred to the ra- dius vector rather than to the $\vec{k}$-vector. It has been pointed out elsewhere, however, that both these models provide the same transition probabilities if one confines oneself to the case of Born's approximation [4].

$$f^{J';F';M'}_{J,F,M}(\beta,\gamma) = \sqrt{\frac{2}{3}} \sum_{\substack{m_I,m_J=M-m_I \\ m'_I,m'_J=M'-m'_I}} (I\ m_I\ Jm_J\,|\,FM)(Im'_I\ J'm'_J\,|\,F'M')\,\delta_{m_I,m'_I} \cdot$$

$$\cdot \sum_{\substack{m_s\quad m_1=m_J-m_s \\ m'_s\quad m'_1=m'_J-m'_s}} (s\ m_s1m_1\,|\,Jm_J)(s\ m'_s\ 1\ m'_1\,|\,J'm'_J)\,\delta_{m_s,m'_s}\cdot(e^{i(\eta^\sigma-\eta^\pi)}-1)\cdot \tag{1}$$

$$(-1)^{m'_l}\,e(1-m'_1\ 1m_1\,|\,2m_1-m'_1)\,C^2_{m_1-m'_1}(\beta,-\gamma)$$

## T A B L E 1

Relative collision-induced transition probabilities among the $^2P$ - sublevels of an alkali atom without nuclear spin. Both the $J = 1/2$ and the $J = 3/2$ level are assumed to be very close to each other

| $m_{J'}$ \ $m_J$ | $\frac{3}{2}$ | $\frac{1}{2}$ | $-\frac{1}{2}$ | $-\frac{3}{2}$ | $\frac{1}{2}$ | $-\frac{1}{2}$ |
|---|---|---|---|---|---|---|
| | $J = \frac{3}{2}$ | | | | $J = \frac{1}{2}$ | |
| $\frac{3}{2}$ | $\frac{27}{45}$ | $\frac{4}{45}$ | $\frac{4}{45}$ | $0$ | $\frac{2}{45}$ | $\frac{8}{45}$ |
| $\frac{1}{2}$ | $\frac{4}{45}$ | $\frac{27}{45}$ | $0$ | $\frac{4}{45}$ | $\frac{4}{45}$ | $\frac{6}{45}$ |
| $-\frac{1}{2}$ ($J = \frac{2}{3}$) | $\frac{4}{45}$ | $0$ | $\frac{27}{45}$ | $\frac{4}{45}$ | $\frac{6}{45}$ | $\frac{4}{45}$ |
| $-\frac{3}{2}$ | $0$ | $\frac{4}{45}$ | $\frac{4}{45}$ | $\frac{27}{45}$ | $\frac{8}{45}$ | $\frac{2}{45}$ |
| $\frac{1}{2}$ ($J = \frac{1}{2}$) | $\frac{2}{45}$ | $\frac{4}{45}$ | $\frac{6}{45}$ | $\frac{8}{45}$ | $\frac{25}{45}$ | $0$ |
| $-\frac{1}{2}$ | $\frac{8}{45}$ | $\frac{6}{45}$ | $\frac{4}{45}$ | $\frac{2}{45}$ | $0$ | $\frac{25}{45}$ |

through a spherical harmonic $C^2$ of rank $(m_1-m_1')$. This function provides the conservation of angular momentum as it carries away the quanta of angular momentum delivered by the transition. In order to obtain relative transition probabilities for the case of collisions under random directions of $\vec{k}$ one has to average the absolute square of $f$ over the whole range of $\beta$, $\gamma$. This provides the list of transition probabilities shown at table 1. concerning the case of zero nuclear spin. Note that transitions would not occur if the initial $m_J$ and the final $m_J'$ differ only with respect to their sign. This is predicted by a selection rule first given by Franz [3]. It holds severely only if $j$ remains a good quantum number during the collision. This is not the case under consideration as we are dealing with Hund's case b where spin and orbit are decoupled by the strength of the molecular field. Therefore, we cannot expect that this selection rule holds in our case generally but only to the scope of Born's approximation. Any better approximation which accounts for stronger dephasing of the $\sigma$- and the $\pi$-states would predict that these transitions should really occur. Formulae of their amplitudes have been derived by the author [4]. But they are not very helpful in calculating relative transition probabilities as they depend strongly on the scattering potential which is, of course, not accurately known. It is the advantage of the transition probabilities shown here that they are independent of the potential specifications other than its splitting into $\sigma$- and $\pi$-branches. Table 2. has been calculated for the actual case of sodium, $I = 3/2$, using also formula (1). Therefore, they hold within the same restrictions as have been quoted for the case $I = 0$.

## Solution of the rate-equation system

By means of these transition probabilities the rate equation system-formulae (2) and (3) - describing optical pumping with $\sigma^+$ -$D_2$-light has been set up.

$$\frac{d\rho_i}{dt} = - \frac{\rho_i}{\tau} - \rho_i N v_r \sum_j \sigma_{i \to j}$$
$$+ N v_r \sum_j \sigma_{j \to i} \rho_j + \sum_I B_{I \to i} u_{I \to i} P_I, \tag{2}$$

T A B L E   2

Relative collision-induced transition probabilities of an alkali atom with nuclear spin I = 3/2 and the J = 1/2 − and the J = 3/2 − level being closely spaced

| F,M_F \ F,M_F | $J=\frac{3}{2}$ | | | | | | | | | | | | | | | | $J=\frac{1}{2}$ | | | | | | | |
|---|---|---|---|---|---|---|---|---|---|---|---|---|---|---|---|---|---|---|---|---|---|---|---|---|
| | 3,3 | 3,2 | 2,2 | 3,1 | 2,1 | 1,1 | 3,0 | 2,0 | 1,0 | 0,0 | 1,-1 | 2,-1 | 3,-1 | 2,-2 | 3,-2 | 3,-3 | 2,2 | 2,1 | 1,1 | 2,0 | 1,0 | 1,-1 | 2,-1 | 2,-2 |
| 3,3 | 2700 | 200 | 200 | 80 | 200 | 120 | 0 | 0 | 0 | 0 | 0 | 0 | 0 | 0 | 0 | 0 | 200 | 200 | 600 | 0 | 0 | 0 | 0 | 0 |
| 3,2 | 200 | 2500 | 200 | 120 | 0 | 80 | 160 | 200 | 0 | 0 | 0 | 0 | 0 | 0 | 0 | 0 | 200 | 300 | 100 | 200 | 200 | 0 | 0 | 0 |
| 2,2 | 200 | 200 | 2500 | 120 | 80 | 80 | 40 | 0 | 160 | 200 | 0 | 0 | 0 | 0 | 0 | 0 | 200 | 0 | 400 | 200 | 200 | 0 | 0 | 0 |
| 3,1 | 80 | 120 | 120 | 2572 | 80 | 48 | 16 | 0 | 64 | 0 | 8 | 120 | 192 | 0 | 0 | 0 | 120 | 320 | 0 | 320 | 80 | 40 | 120 | 0 |
| 2,1 | 200 | 0 | 80 | 80 | 2500 | 120 | 160 | 0 | 40 | 200 | 80 | 0 | 0 | 0 | 0 | 0 | 300 | 50 | 150 | 50 | 50 | 100 | 300 | 0 |
| 1,1 | -120 | 80 | 80 | 48 | 2532 | 2532 | 24 | 120 | 96 | 0 | 192 | 80 | 120 | 0 | 0 | 0 | 180 | 30 | 250 | 30 | 270 | 60 | 180 | 0 |
| 3,0 | 0 | 160 | 40 | 16 | 160 | 24 | 2628 | 0 | 72 | 0 | 24 | 160 | 120 | 0 | 200 | 0 | 40 | 250 | 30 | 360 | 0 | 30 | 250 | 40 |
| 2,0 | 0 | 200 | 0 | 80 | 0 | 120 | 0 | 2500 | 0 | 200 | 120 | 160 | 0 | 160 | 0 | 0 | 200 | 200 | 0 | 0 | 200 | 200 | 0 | 200 |
| 1,0 | 0 | 0 | 160 | 64 | 40 | 96 | 72 | 0 | 2628 | 0 | 96 | 40 | 16 | 40 | 160 | 0 | 360 | 0 | 120 | 40 | 0 | 120 | 0 | 360 |
| 0,0 | 0 | 0 | 200 | 0 | 200 | 0 | 0 | 200 | 0 | 2500 | 0 | 200 | 0 | 200 | 0 | 0 | 200 | 50 | 150 | 0 | 200 | 150 | 50 | 200 |
| 1,-1 | 0 | 0 | 0 | 8 | 80 | 192 | 24 | 120 | 96 | 0 | 2532 | 80 | 120 | 80 | 120 | 120 | 180 | 300 | 60 | 30 | 270 | 250 | 30 | 180 |
| 2,-1 | 0 | 0 | 0 | 120 | 0 | 80 | 160 | 160 | 40 | 200 | 80 | 2500 | 80 | 0 | 120 | 200 | 300 | 300 | 100 | 50 | 50 | 150 | 300 | 0 |
| 3,-1 | 0 | 0 | 0 | 192 | 0 | 120 | 120 | 0 | 16 | 0 | 120 | 80 | 2572 | 120 | 200 | 80 | 0 | 0 | 40 | 320 | 80 | 50 | 50 | 0 |
| 2,-2 | 0 | 0 | 0 | 0 | 0 | 0 | 0 | 160 | 40 | 200 | 80 | 0 | 120 | 2500 | 200 | 200 | 0 | 0 | 0 | 200 | 200 | 400 | 0 | 200 |
| 3,-2 | 0 | 0 | 0 | 0 | 0 | 0 | 200 | 0 | 160 | 0 | 120 | 120 | 200 | 200 | 2500 | 200 | 0 | 0 | 0 | 200 | 200 | 0 | 300 | 200 |
| 3,-3 | 0 | 0 | 0 | 0 | 0 | 0 | 0 | 0 | 0 | 0 | 120 | 200 | 80 | 200 | 200 | 2700 | 0 | 0 | 0 | 0 | 0 | 0 | 0 | 0 |
| 2,2 | 200 | 200 | 600 | 0 | 300 | 180 | 40 | 200 | 360 | 200 | 180 | 300 | 0 | 0 | 0 | 0 | 2500 | 0 | 0 | 0 | 0 | 0 | 0 | 0 |
| 2,1 | 200 | 300 | 100 | 320 | 50 | 30 | 250 | 200 | 0 | 50 | 300 | 50 | 0 | 0 | 0 | 0 | 0 | 2500 | 0 | 0 | 0 | 0 | 0 | 0 |
| 1,1 | 600 | 100 | 400 | 0 | 150 | 250 | 30 | 0 | 120 | 150 | 60 | 100 | 40 | 0 | 0 | 0 | 0 | 0 | 2500 | 0 | 0 | 0 | 0 | 0 |
| 2,0 | 0 | 200 | 200 | 320 | 50 | 30 | 360 | 0 | 40 | 0 | 30 | 50 | 320 | 200 | 200 | 0 | 0 | 0 | 0 | 2500 | 0 | 0 | 0 | 0 |
| 1,0 | 0 | 200 | 200 | 80 | 50 | 270 | 0 | 200 | 0 | 200 | 270 | 50 | 80 | 200 | 200 | 0 | 0 | 0 | 0 | 0 | 2500 | 0 | 0 | 0 |
| 1,-1 | 0 | 0 | 0 | 40 | 100 | 60 | 30 | 400 | 120 | 150 | 250 | 30 | 0 | 400 | 0 | 600 | 0 | 0 | 0 | 0 | 0 | 2500 | 0 | 0 |
| 2,-1 | 0 | 0 | 0 | 120 | 300 | 180 | 250 | 0 | 0 | 50 | 30 | 300 | 320 | 0 | 300 | 200 | 0 | 0 | 0 | 0 | 0 | 0 | 2500 | 0 |
| 2,-2 | 0 | 0 | 0 | 0 | 0 | 0 | 40 | 200 | 360 | 200 | 180 | 0 | 120 | 200 | 200 | 200 | 0 | 0 | 0 | 0 | 0 | 0 | 0 | 2500 |

Each number divided by 4500

List of collision-induced transition probabilities for an atomic $^2P$-state, the $J = \frac{1}{2}$ − and $J = \frac{3}{2}$ −levels being closely spaced and J being coupled to a nuclear spin I = $\frac{3}{2}$

$$\frac{dP_I}{dt} = - P_I \sum_i B_{I \to i} \; u_{I \to i} \; - (P_I - \frac{1}{8})/T \tag{3}$$

$$+ \sum_i A_{i \to I} \; \rho_i$$

It is divided into two parts, one part consisting of 24 rate equations deals with the population of the excited states. Mind that $\tau$ means the mean lifetime of these states, N the buffer gas density, $v_r$ the mean relative velocity of the colliding atoms, $\sigma_{i \to j}$ the cross section for any transition among excited substates the relative magnitudes of which are shown in table 2, $B_{I \to i}$ means Einstein's B-value for an excitation from ground state I to excited state i, $u_{I \to i}$ the related energetical density of the exciting radiation field. Another part consisting of eight equations deals with the ground state population. The first term accounts for absorption, the second one for relaxation, T being the relaxation time, the third one for spontaneous decay into state I, $A_{i \to I}$ being Einstein's A-value for the denoted transition. The rate equations system has been solved for the stationary case by means of a computer. From the ground state populations thus obtained the relative change of the optical absorption has been calculated according to the equation (4).

$$\frac{\Delta A}{A} = \frac{\sum_{I,i} P_I \; B_{I \to i} \; u_{I \to i}}{\sum_{I,i} B_{I \to i} \; u_{I \to i}} - \frac{1}{8} \tag{4}$$

Fig. 3 shows a plot of the negative of this quantity versus the buffer gas pressure.

The change of the optical absorption is zero if no buffer gas is present because then optical pumping is prevented by the very strong ground state relaxation resulting from the uncoated walls of our pumping cell. With increasing buffer gas pressure the absorption rises and the transparency drops until excited state mixing becomes efficient. Then the change of the absorption is lowered again, passes through zero and approaches strong negative values. At very high pressures not shown by this plot it approaches zero again because of the then dominating volume
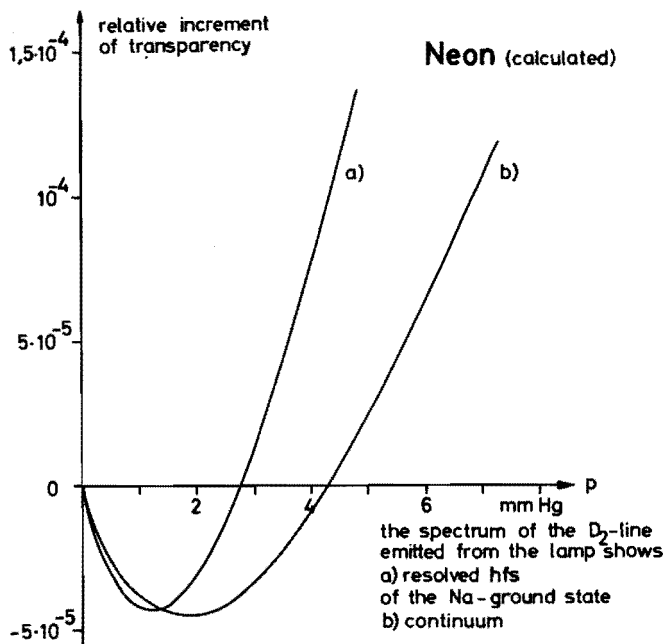
relative increment of transparency

Neon (calculated)

a)

b)

the spectrum of the $D_2$-line emitted from the lamp shows
a) resolved hfs
of the Na-ground state
b) continuum

Fig. 3. Calculated change of the optical absorption of a sodium vapor pumped with $D_2$-light as a function of the buffer gas pressure. The depolarizing cross section for Ne of table 3 has been used in the calculation. The negative of the relative absorption change was plotted versus the buffer gas pressure
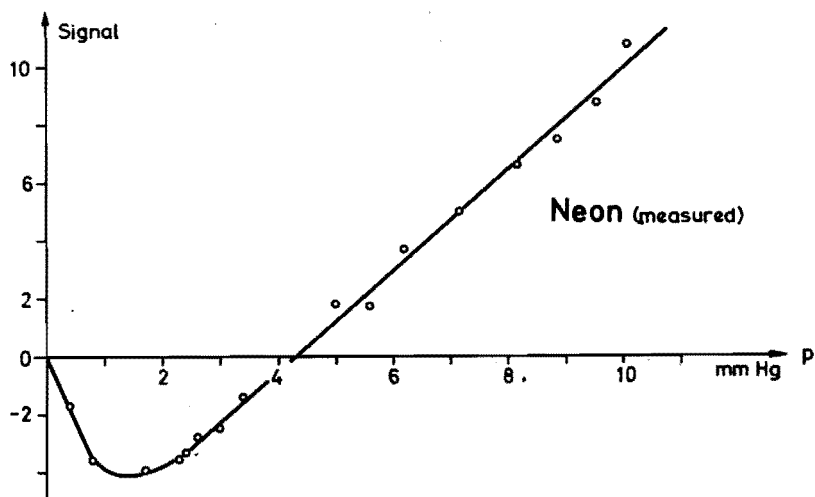


Signal

Neon (measured)

Fig. 4. The measured optical pumping signal as a function of the buffer gas pressure. Neon was used in this case. The optical transparency increases from the bottom to the top
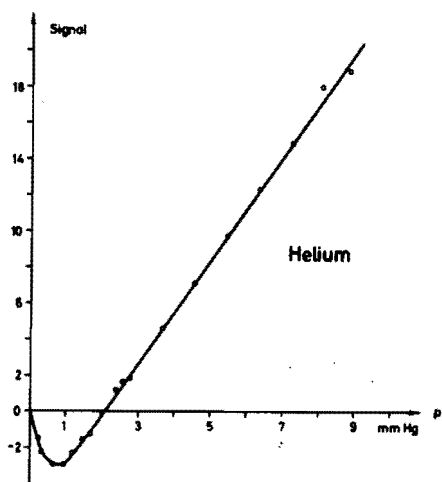
Fig. 5. The optical pumping signal if Helium is used as a buffer gas
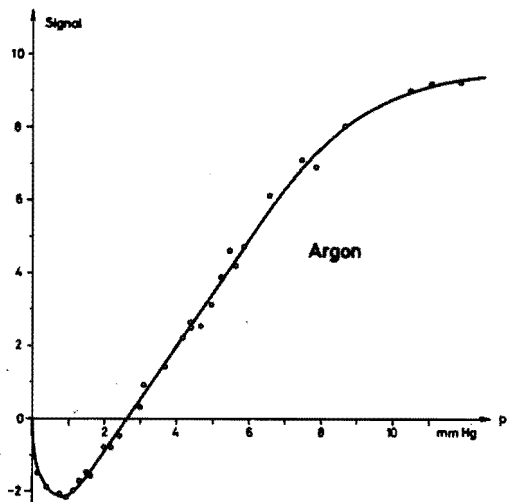
Fig. 6. The optical pumping signal if Argon is used as a buffer gas
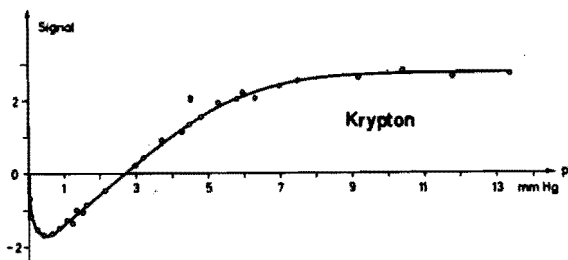


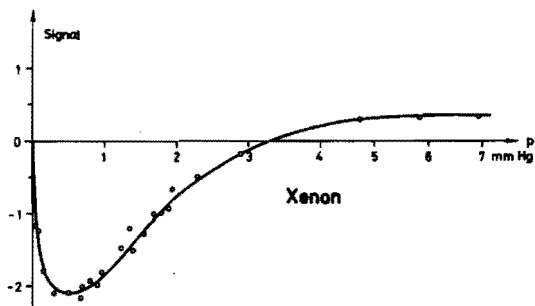Fig. 7. The optical pumping signal if Krypton is used as a buffer gas



Fig. 8. The optical pumping signal if Xenon is used as a buffer gas

relaxation. It was amazing to learn by this plot that the pressures of zero absorption change depend on the lamp's spectral profile.Case a) holds for a lamp emitting a well resolved ground state hyperfine structure. Case b) holds for a lamp emitting a continuum.

## Experimental investigation of the optical pumping signal as a function of buffer gas pressure

Now in order to measure the relative change of absorption caused by optical pumping with $D_2$-light we employed an ordinary apparatus for optical pumping. The lamp was a radio-frequency lamp with the bulb thermostabilized in an oil-bath. In order to select the $D_2$-line from the emitted light a Lyot-filter has been used. The cell was connected to a vacuum apparatus which served for the adjustment of the buffer gas pressure. The polarization of the vapor was periodically disturbed by superposing a strong vertical magnetic field to the horizontal one. The repetition frequency of these disturbances was 8 c/s in order to have the intervals long enough so that repumping to the equilibrium might be possible. The transmitted light was measured by means of a photo-cell. The component of the photo-current which was synchronous to the repetition frequency was detected by a lock-in set. The signals such obtained are plotted versus the buffer gas pressure. In this way the curve for Ne shown by Fig. 4 was obtained exhibiting the zero passing at 4,3 Torr.

Fig. 5-8 show the curves for He with the zero passage at 2.1 Torr, for Ar with the zero at 2.7 Torr, for Kr with with the zero at 2.8 Torr,and for Xe with the zero at 3.3 Torr. Mind that in the case of Kr and even more in the case of Xe the volume relaxation is so strong that just behind the zero passage the curve drops to zero.Thus in the case of Xe the zero can be evaluated only with great inaccuracy,perhaps 20 per cent.In any other case the accuracy should be better than 5 per cent.Next we had to investigate the lamp spectral profile. This was performed by means of photoelectric Fabry-Perot-interferometer Fig.9 shows the $D_2$-line hyperfine spectrum at three different temperatures. The low temperature recording shows the hyperfine structure with weak

**T A B L E  3**

List of the measured depolarizing cross sections. Comparison with values from sensitized fluorescence measurements

| | $P_o$ mm Hg | $T_{lamp}$ °C | $\bar{\sigma}_{FM_F \to F'M'_F}$ Å² uncorrected | $\bar{\sigma}_{FM_F \to F'M'_F}$ Å² corrected for the lamp profile | ratio | $Q_1$ to the Na-Ne Krause value | ratio to the Pitre and Na-Ne value | $Q_1 = 2Q_2 e^{-\frac{\Delta E}{kT}}$ to the Franken and Jordan value | ratio to the Na-Ne value |
|---|---|---|---|---|---|---|---|---|---|
| Na-He | 2,1 | 202 | 112 | 105 | 1,12 | 86,0 | 1,26 | 77 | 1,14 |
| Na-Ne | 4,3 | 202 | 97 | 94 | 1,00 | 67,0 | 1,00 | 68 | 1,00 |
| Na-Ar | 2,7 | 214 | 184 | 160 | 1,7 | 109,9 | 1,64 | 121 | 1,80 |
| Na-Kr | 2,8 | 214 | 197 | 173 | 1,84 | 85,0 | 1,27 | 128 | 1,90 |
| Na-Xe | 3,3 | 216 | 174 | 141 | 1,5 | 89,8 | 1,34 | 116 | 1,72 |

self reversal, the high temperature recording shows strong self reversal as a replica of the positive hyperfine structure is missing in the line centre. The case of a continuum has been found to be realized approximately at 194 degrees Celsius. Care has been taken that the lamp temperature was not too far from this value during the pumping experiment. It was found out, of course, that the pressure of the zero absorption change is dependent on the lamp temperature.

Fig.10 shows how the zeros are shifted as the lamp temperature changes. A theoretical prediction was also made by inserting the measured ratio of intensities of the hyperfine components into our rate equation system solving it afterwards by the computer. The predicted and the measured curves are well resembling each other.

Table 3 gives in the first column the collision partners, in the second one the pressures of zero absorption change, in the
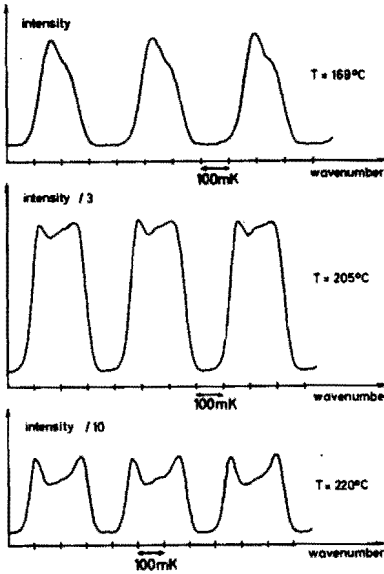


Fig. 9. The hyperfine spectrum of the $D_2$-line emitted from a radio frequency lamp at different temperatures
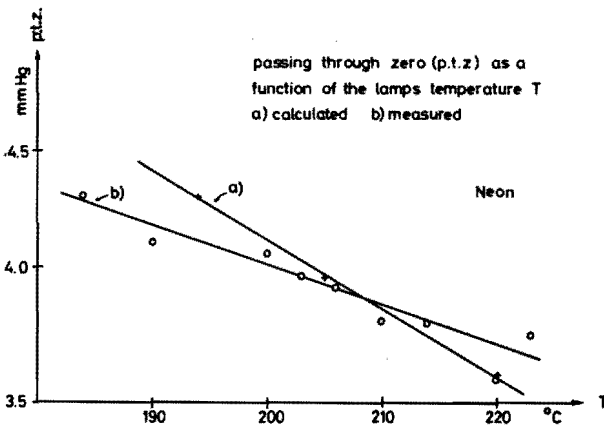


Fig.10. The shift of the pressure of zero absorption change as a function of the lamp temperature

third one the mixing cross sections derived from the latter ones by means of the formula

$$N \; v_r \; \overline{\sigma}_{FM_F \to F'M_F'} = 1 \cdot 446/\tau. \tag{5}$$

which was obtained from the rate equation system (2) and (3) by numerical methods. It holds only for the pumping light spectrum being a continuum $\overline{\sigma}_{FM_F \to F'M_F'}$ is defined in the following way

$$\overline{\sigma}_{FM_F \to F'M_F'} = \frac{1}{(2I+1)(2J+1)} \sum_{F,M_F} \sum_{F',M_F', \neq F,M_F} \sigma_{FM_F \to F'M_F'} \tag{6}$$

that means by summing $\sigma_{FM_F \to F'M_F'}$ over the final states and averaging it afterwards over the initial states. In the fourth column the mixing cross-sections are given, corrected for the spectral profile deviations from the continuum. In the fifth and the sixth column the cross sections $Q_1$ for transitions from $^2P_{1/2}$ to $^2P_{3/2}$ are given as communicated by the quoted authors [5,6]. They originate from sensitized fluorescence measurements. The relative sizes of our cross-sections agree better with those of Franken and Jordan [4] than with those of Pitre and Krause [6]. The absolute size of our cross-sections may be also comparable to $Q_1$ in so far as no direct mixing occurs among the $^2P_{1/2}$-sublevels. Otherwise our cross sections should be even higher. But note that we have made certain assumptions which would not hold in practice. For instance the hyperfine splitting of $3\,^2P_{3/2}$ is of the same order of magnitude as the width of these levels due to spontaneous decay. Therefore, the basis set of hyperfine states $|FM_F\rangle$ so far used may be not the proper one because these states do not live during even one period of the precession of I and J around their resultant F. Therefore, concerning $3\,^2P_{3/2}$ a basis set of decoupled hyperfine states $|M_I M_J\rangle$ would be suitable to our consideration, too. This has not yet been undertaken.

Larmor resonance $\Delta M_F=1, \Delta F = 0$ under the conditions of $D_2$-light-pumping

Finally let us consider the results of measurements where the polarization of the vapour was disturbed by a radio-frequency magnetic field instead of a vertical constant magnetic field. Fig. 11 shows the measured Larmor resonances at 1,2 Mc/s with the buffer gas pressure being in two cases smaller and in one
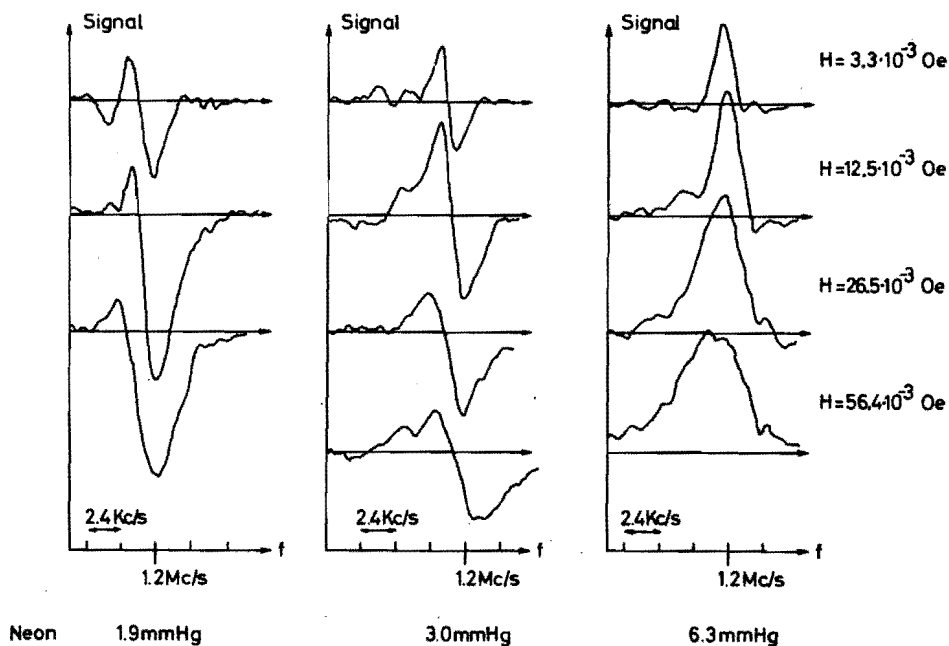


Fig. 11. Larmor resonances observed in the transmitted pumping light at different Neon pressures and at different radio frequency field strengths

case higher than the value of zero passage and the amplitude of the radio frequency field increasing from up to down. There are apparently two closely spaced resonances the left of which can be ascribed to the Larmor resonances of the ground state f = 1 level whereas the right one can be ascribed to the ground state f = 2 level. The first one remains always positive whereas the second one inverses its sign. This behaviour is well explained

by the steady state solution of our pumping rate equation system. Fig.12 shows the eight Zeeman sublevels of the ground state with their calculated populations drawn in. This is just the case of zero absorption change. If you equalize the populations of any

two neighbouring levels you will get decreasing absorption in the case of the f=2 levels and increasing absorption in the case of the f = 1 levels. The thus calculated spectrum of Larmor resonances is shown in Fig. 13. This is the case of low rf-intensity.Unfortunately, as we have seen, the ratio of the positive and the negative signal is dependent on the rf-intensity. Therefore, no unique method of ascertaining excited state mixing cross sections is provided by the measurement of Larmor resonances.
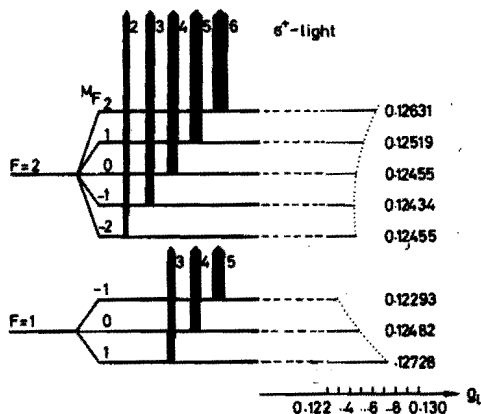


Fig. 12. Population of the eight ground-state sublevels.In this case the optical absorption is the same as it would be in the case of random distribution
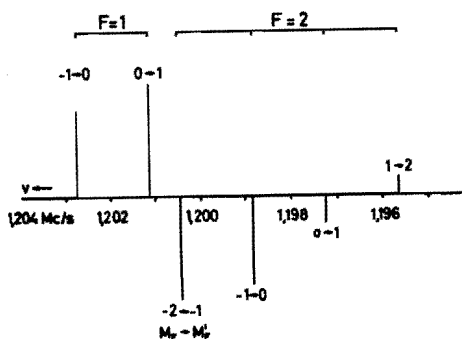


Fig. 13. Spectrum of the resonances $\Delta F = 0, \Delta M_F = \pm 1$ as has been calculated from the distribution of Fig. 12

## Acknowledgements

R E F E R E N C E S

[1] M. Elbel and F. Naumann, Zs. Phys., 204, 501 (1967).
    Erratum in               Zs. Phys., 204, 501 (1967).
[2] J. Fricke, J. Haas, E. Lüscher and F.A. Franz, Phys.Rev.,163,45 (1967)
[3] F. A. Franz, G. Leutert, and R. T. Shuey, Helv. Phys. Acta, 40, 778
    (1967).
[4] M. Elbel, to be published in Ann. der Phys.
[5] J. A. Jordan and P. A. Franken, Phys. Rev., 142, 20 (1966).
[6] J. Pitre and L. Krause, Canad. J. Phys., 45, 2671 (1967).

D i s c u s s i o n

F. A. Franz

It is often assumed that by adding sufficient noble gas to the
lamp, say 8 or 10 Torr, that a broad and flat profile with-
out resolved hyperfine structure will be obtained. Can you, or
anyone alse in the audience give definite information on this
point.

M. Elbel

No systematic investigation of this point has been done. Our
bulbs contained only 1 Torr Argon in any which is perhaps not
sufficient to provide flat lamp profiles. But we should make use
of your suggestion in the future.

J. Fricke

Did you check the influence of the changed pumping light in-
tensity on the pass through zero of $\langle S_z \rangle$ when you altered
the lamp profile?

## M. Elbel

As the relaxation in the ground state is very strong because of the uncoated glass-walls all the ground state sublevels should be nearly equally populated. Calculations show in this case that the pressures of the passing through zero would not depend on the lamps absolute intensity but only on the relative intensity of the hyperfine components.